Reducing Mg Anode Overpotential via Ion Conductive Surface Layer Formation by Iodine Additive

Xiaogang Li, Tao Gao, Fudong Han, Zhaohui Ma, Xiulin Fan, Singyuk Hou, Nico Eidson, Weishan Li, and Chunsheng Wang**

Electrolytes that are able to reversibly deposit/strip Mg are crucial for rechargeable Mg batteries. The most studied complex electrolytes based on Lewis acid-base chemistry are expensive, difficult to be synthesized, and show limited anodic stability. Conventional electrolytes using simple salts such as $Mg(TFSI)_2$ can be readily synthesized, but Mg deposition/stripping in these simple salt electrolytes is accompanied by a large overpotential due to the formation of a surface layer on the Mg metal with a low Mg ion conductivity. Here the overpotential for Mg deposition/stripping in a simple salt, $Mg(TFSI)_2$-1,2-dimethoxyethane (DME), electrolyte is significantly reduced by adding a small concentration of iodine ($\leq 50 \times 10^{-3}$ M) as an additive. Mechanism studies demonstrate that an Mg ion conductive solid MgI_2 layer is formed on the surface of the Mg metal and acts as a solid electrolyte interface. With the $Mg(TFSI)_2$-DME-I_2 electrolyte, a very small voltage hysteresis is achieved in an Mg-S full cell.

The rechargeable magnesium battery (RMB) has attracted extensive attention recently because of several unique advantages. Magnesium metal has a low reduction potential (−2.36 V vs normal hydrogen electrode (NHE)), high theoretical gravimetric capacity (2205 mA h g^{-1}) and volumetric capacity (3833 mA h cm^{-3}), high natural abundance in the earth's crust, and is less sensitive to moisture and air than alkali metals (such as Li, Na, etc.).[1,2] Furthermore, there is no dendrite formation on the Mg surface during the charge/discharge process, which eliminates the safety concern of internal shorts in rechargeable metal batteries like the Li metal battery. However, two critical challenges impede the development of RMBs. One challenge is the sluggish diffusion of the bivalent Mg ion in the cathode host structures, which generates large overpotentials for Mg intercalation[3–5] and greatly hinders the development of practical cathode materials for RMBs.[6,7]

Dr. X. Li, Dr. T. Gao, Dr. F. Han, Dr. Z. Ma, Dr. X. Fan, Dr. S. Hou, Dr. N. Eidson, Prof. C. Wang
Department of Chemical and Bimolecular Engineering
University of Maryland
College Park, MD 20740, USA
E-mail: cwang@umd.edu
Dr. X. Li, Prof. W. Liv
College of Materials Science and Engineering
South China University of Technology
Guangzhou 510641, China
E-mail: liwsh@scnu.edu.cn

DOI: 10.1002/aenm.201701728

Another challenge is the development of electrolytes that can effectively utilize an Mg metal anode. Extensive effort has been put in to develop electrolytes capable of reversibly depositing/stripping Mg. Most work has focused on complex electrolytes that allow fast and reversible Mg deposition/stripping. Such electrolytes were first proposed by Aurbach's group in 2000,[8] and subsequently they developed the all phenyl complex showing high anodic stability.[9] Later, a non-nucleophilic electrolyte, Mg-HMDS, was developed by Muldoon and co-workers, and Fichtner and co-workers for Mg/S batteries.[10,11] To eliminate the organic Grignard species in the electrolyte, an all inorganic electrolyte, magnesium aluminum chloride complex, was reported.[12–15] These complex electrolytes have enabled the usage of Mg-cathode half-cells to evaluate various cathode materials due to their capability of facile Mg deposition/stripping;[8,10,16–18] however, their complicated synthesis procedure, incompatibility with oxide cathodes, sensitivity to air and moisture, low ionic conductivity, and high cost have rendered them less attractive for practical applications than conventional organic electrolytes based on simple salts (salts containing anions of PF_6^-, BF_4^-, $TFSI^-$, etc.). Unfortunately, most of these simple salt electrolytes are not compatible with Mg metal because poorly or nonconductive surface layers are normally formed on the Mg surface. In the electrolytes based on common aprotic organic solvents (such as AN, PC, etc.), the surface film is dominated by the decomposition of solvent due to their weak reduction stability, and the formed layer can block the deposition/stripping of Mg.[19] Even for solvents that are stable with Mg metal (such as glyme), the decomposition of salts or the reaction of trace moisture with Mg can still form a surface film covering the Mg surface, leading to a large overpotential for Mg deposition/stripping.[20–23] Therefore, the formation of a poorly or even nonconductive surface layer on Mg metal in common simple salt organic electrolytes is inevitable due to Mg's strong reducing ability, which remains a challenge for the application of a Mg metal anode in these simple salt electrolytes. Herein, we propose for the first time a facile approach to solve this problem by tuning the composition of the surface layer and forming an Mg ion conductive layer. By adding a small concentration of iodine ($<50 \times 10^{-3}$ M) into the electrolyte, an insoluble magnesium iodide layer is formed on the surface of the Mg metal, which acts as a solid electrolyte

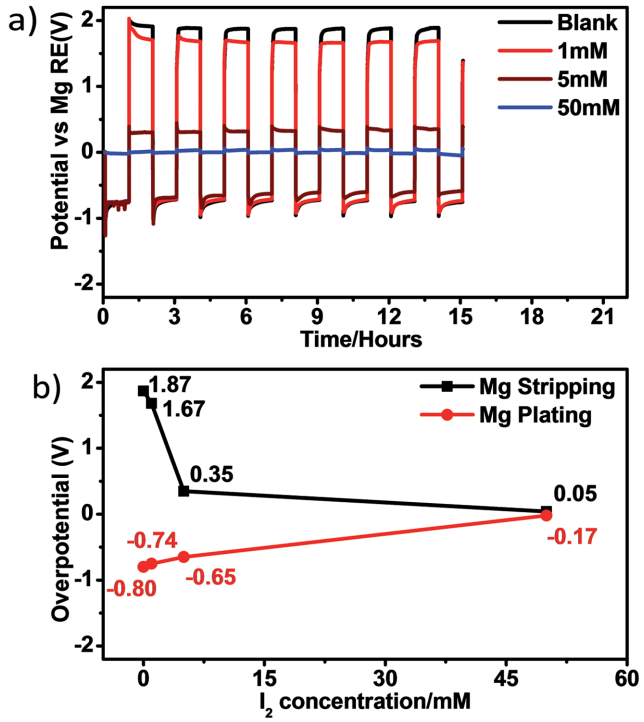

Figure 1. Mg stripping/deposition overpotential in Mg/Mg/Mg T-cell in the 0.5 M $Mg(TFSI)_2$-DME electrolytes with different amount of I_2 additives. a) Potential of Mg electrode during cycling; b) overpotentials for deposition and stripping. Current density: 1.41 mA cm^{-2}.

interface (SEI) that reduces the overall Mg anode overpotential, instead of as a passivation layer. Utilizing this electrolyte, we demonstrate that the huge voltage hysteresis, commonly observed in RMBs with simple salt electrolytes, can be significantly decreased to a much more practical level.

The Mg stripping/deposition overpotential in the 0.5 M $Mg(TFSI)_2$-1,2-dimethoxyethane (DME) electrolyte was measured in a three-electrode cell using three Mg disks as working electrode (WE), counter electrode (CE), and reference electrode (RE) (Figure S1, Supporting Information). The potential of Mg during Mg stripping/deposition cycling is shown in **Figure 1**a. Consistent with previous studies,[24,25] a large stripping overpotential (≈1.87 V) and deposition overpotential (≈–0.8 V) can be observed in the blank electrolyte (no iodine). After the addition of a small amount of iodine, the overpotentials for both Mg stripping and deposition decline, and decrease more with increasing concentration of iodine additives. The relationship is shown in Figure 1b, which clearly demonstrates the reducing overpotential with the iodine additive. The stripping/deposition overpotential decreases to 1.67 and –0.74 V with 1×10^{-3} M iodine, respectively. When the iodine concentration increases to 5×10^{-3} M, the overpotentials for deposition/stripping abruptly decrease to 0.35 and –0.65 V, respectively. Further increasing the iodine concentration to 50×10^{-3} M results in both stripping and deposition, and overpotentials becoming negligible, 0.05 and –0.17 V, respectively. These results demonstrate that the presence of a small amount of iodine in 0.5 M $Mg(TFSI)_2$-DME electrolyte can significantly reduce the overpotential for Mg deposition/stripping.

To understand the mechanism underlying this unique phenomenon, we first examined the surface morphology and chemistry of Mg electrodes. Mg electrodes were thoroughly washed and rinsed with DME to remove any soluble species before characterization. Mg electrodes aged in electrolytes with different iodine concentrations were examined using scanning electron microscopy (SEM) and energy dispersive X-ray spectroscopy (EDS) (Figure S2, Supporting Information). No apparent morphology change is observed and EDS shows no iodine signal when iodine concentration is $\leq 50 \times 10^{-3}$ M. However, micron-sized solids with tree-like structures appear with a strong iodine signal in EDS when the iodine concentration reaches 100×10^{-3} M. This result indicates that at high iodine concentrations ($\geq 100 \times 10^{-3}$ M) the dissolved iodine reacts vigorously with the Mg surface, while no MgI_2 can be found at lower iodine concentrations within the detection limits of EDS. To obtain a finer picture of the surface chemistry of the Mg electrodes in the electrolytes with low iodine concentrations, we performed X-ray photoelectron spectroscopy (XPS). C, O, S, N, F, and Mg elemental signals can be found for the Mg electrode recovered from the blank electrolyte (Table S1, Supporting Information), among which S, N, and F must arise from the decomposition of the $TFSI^-$ anion.[22,23] These species are not likely to form a thick surface layer covering the Mg electrode, because the high resolution Mg 2p spectrum shows a Mg^0 peak (**Figure 2**) that agrees with previously reported XPS analyses of

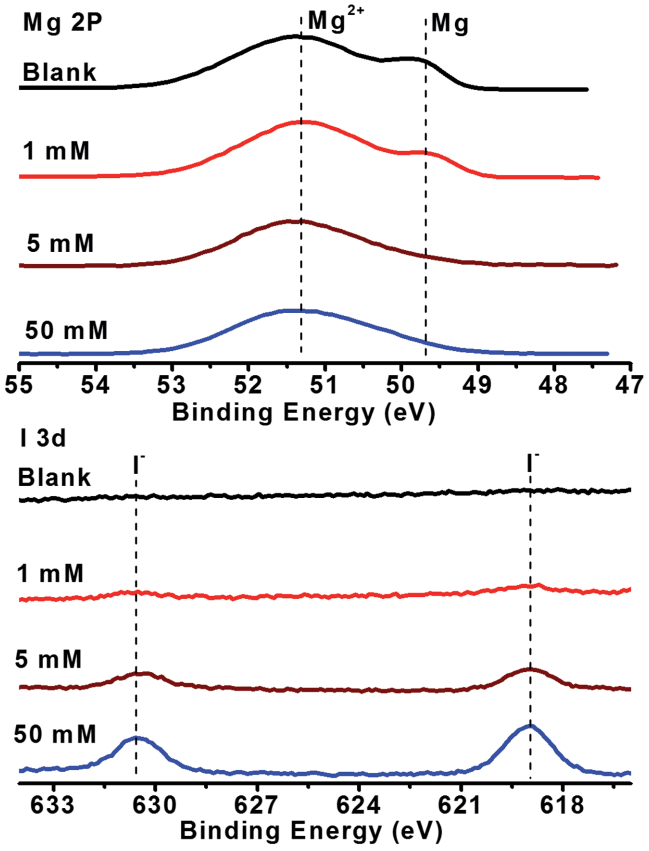

Figure 2. High resolution Mg 2p and I 3d spectra of cycled Mg in electrolytes with different concentrations of iodine. All spectra are plotted on the same intensity range.

Mg anodes in the same electrolyte.[22,26] According to a previous systematic XPS study of Mg metal, this surface layer could only be a few nanometer thick.[27] Thin though it is, the presence of such a surface layer possess larger barriers for Mg deposition/stripping. After the addition of iodine, an I elemental signal appears on the Mg surface (Table S1, Supporting Information) accompanied by the appearance of an I^- peak in the high resolution I 3d spectrum (Figure 2), indicating the formation of a MgI_2 layer. The growing intensity of the I^- peak and disappearance of the Mg^0 peak suggests that the surface layer grows thicker at higher iodine concentrations ($\geq 5 \times 10^{-3}$ M). XPS depth profiles were further collected (Figure S3, Supporting Information) and after 36 min of sputtering, the Mg^0 peak reappears and the I^- peak disappears, indicating the removal of this surface layer. These XPS results imply that a dense insoluble surface layer containing MgI_2 is formed on the Mg electrode in electrolytes with iodine concentrations $>5 \times 10^{-3}$ M. Since MgI_2 has a high ionic conductivity but low electronic conductivity,[17,28] this surface layer is highly likely to behave as a SEI.

To examine how this surface layer affects the interfacial resistance of the Mg anode, we measured the electrochemical impedance spectroscopy (EIS) of Mg anode in the three-electrode cell using Mg as RE and CE in the different electrolytes (**Figure 3**). The Nyquist plot in the blank electrolyte is characterized by a depressed but symmetric semicircle (Figure 3a), corresponding to interfacial resistance. Its large value (≈275 kΩ) illustrates the very poor interfacial reaction kinetics for the deposition/stripping reaction. With the addition of iodine, the Nyquist plot starts to deform and loses its symmetry (Figure 3b–d). This indicates that a new interfacial process emerges which alters the shape of the Nyquist plot. To identify and separate this new physical process, we fit the EIS data with the equivalent electrical circuit shown in Figure 3e, in which two R–C pairs are used. The fitted curve (black) well captures the experimental results (black circles). The two R–C pairs are plotted separately on the Nyquist plots with their characteristic frequencies labelled. Since Mg ion migration through surface layers precedes the charge transfer process in the anode reaction, the red semicircles with high characteristic frequency (100 Hz) correspond to ion migration in the SEI and the blue semicircles with low characteristic frequency (1 Hz) correspond to charge transfer. The fitted data is summarized in Table S2 (Supporting Information). The ohmic resistances are similar in all electrolytes (≈240 Ω). However, the overall interfacial resistances (R_{ct} and R_{SEI}) drop by three orders of magnitude, from 275 kΩ in the blank electrolyte to 320 Ω in the electrolyte with 50×10^{-3} M iodine additive, which explains the reduced overpotential for Mg deposition/stripping. The decrease in R_{ct} suggests that the reduction of the Mg ion is facilitated. Because the Mg ion reduction is a two-step process, the enhanced kinetics

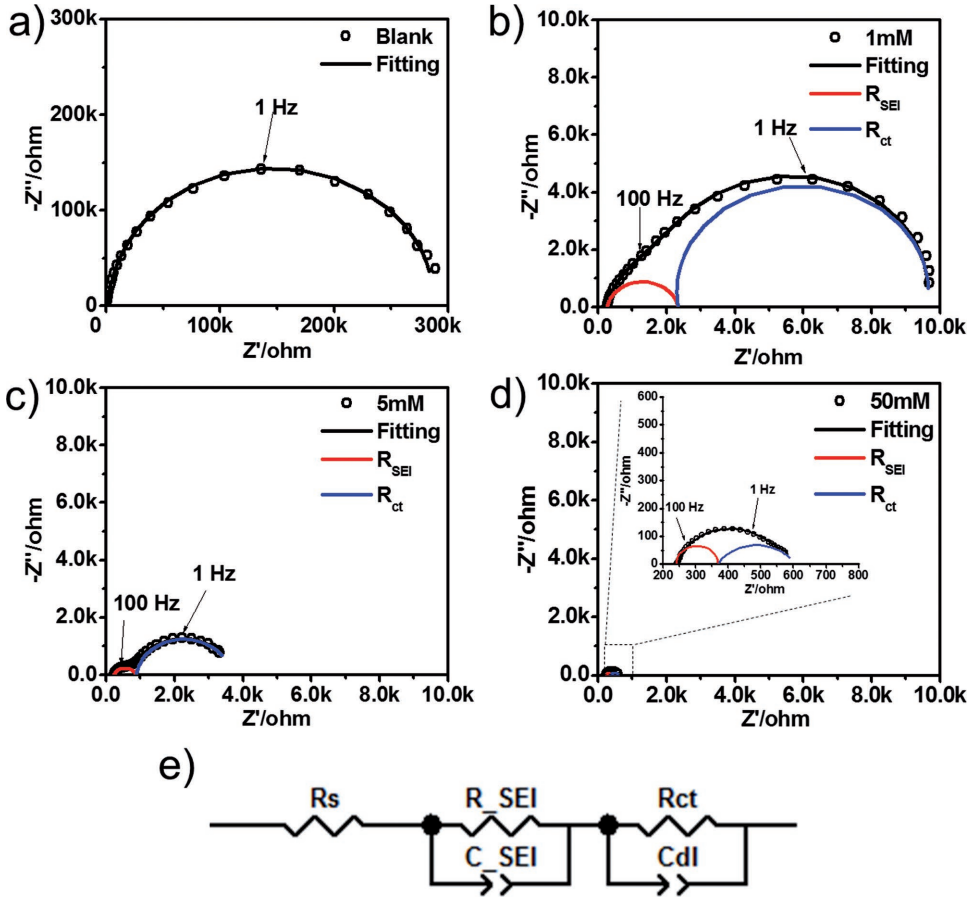

Figure 3. The EIS of Mg electrode cycled in blank electrolyte and electrolytes with different concentrations of iodine. a) blank, b) 1×10^{-3} M, c) 5×10^{-3} M, d) 50×10^{-3} M. Inset: zoom-in region. e) Equivalent circuits to fit the EIS data.

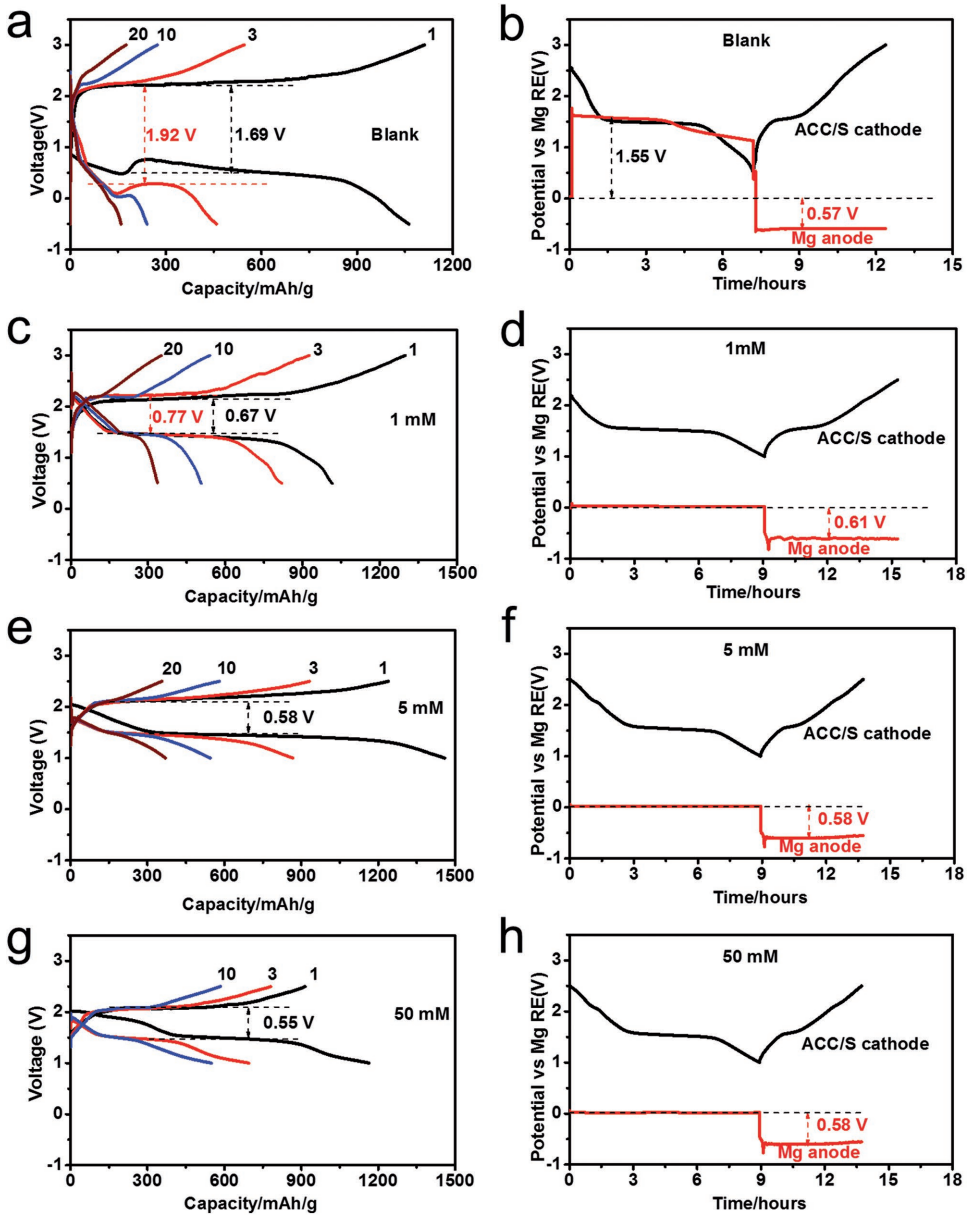

Figure 4. a,c,e,g) The charge/discharge curves of Mg/S full cell in the blank electrolyte and electrolytes containing iodine. Current density: 168 mA g^{-1}. All the curves are plotted in the same voltage range for comparison. b,d,f,h) The potential of sulfur working electrode (WE) and Mg counter electrode (CE) versus Mg reference electrode (RE) in a three-electrode cell in the blank electrolyte and electrolytes containing iodine. Current density: 84 mA g^{-1}.

is probably a result of a lowered energy of the transient state (Mg^{+}) due to the presence of iodide.

Although the above experimental results provide direct evidence of the reduced overpotential of the Mg electrode during its operation, it remains unknown how iodine impacts the cathode, i.e., whether such electrolytes can enable the operation of an Mg full cell. To answer this question, we assembled and tested Mg/S full cells (anode: Mg, cathode: S) with both the blank electrolyte and electrolytes containing iodine (**Figure 4**). The typical charge/discharge voltage profiles of the Mg/S full cells were plotted in the same voltage range (Figure 4a,c,e,g). A large voltage hysteresis of 1.69 V is observed in the blank electrolyte (Figure 4a), agreeing with previous reports.[29] The discharge voltage plateau is 0.5 V during the first cycle, which significantly deviates from the thermodynamic electromotive force (emf) of sulfur (1.77 V) in Mg/S chemistry.[16] Such large voltage hysteresis, also reported in previous studies using the same electrolyte,[29–31] is detrimental to fully utilize the theoretical energy of the battery because such hysteresis significantly compromises the energy efficiency of the system. In sharp contrast, the Mg/S full cells with iodine additive show remarkably reduced voltage hysteresis, and the discharge plateau is at ≈1.5 V, closer to sulfur's emf and consistent with Mg/S full cells using complex electrolyte where the Mg anode is free of any surface layer.[16,32] The significantly reduced voltage hysteresis was explained by electrochemical results obtained from a

Mg/Mg/S three-electrode cell, in which the potential of the S cathode and Mg anode was recorded versus Mg RE. The potentials of sulfur cathodes are comparable in all cells (1.6 V), close to its theoretical potential. Furthermore, there is one more redox pair at ≈2.0 V corresponding to I_2/MgI_2 with increasing concentration of iodine. However, a huge discrepancy was seen regarding the potential of the Mg anode: in electrolytes containing iodine there is almost no overpotential for Mg stripping, while a huge overpotential of 1.55 V is seen in the blank electrolyte. It demonstrates that the reduced voltage hysteresis in the Mg/S full cell is largely ascribed to the small Mg stripping overpotential in electrolytes containing iodine. Together, these electrochemical results show that the iodine containing electrolyte renders a clearly reduced voltage hysteresis, hence the higher energy efficiency for the Mg/S full cell. It is noted that the Mg deposition/striping is not symmetrical in overpotential in the iodine containing electrolyte. A similar phenomenon is also observed on other $Mg(TFSI)_2$ containing electrolytes,[25] and we speculate it has to do with the structure of the Mg cation in the electrolyte and the asymmetry of the redox reaction of Mg^{2+}/Mg^0.

In conclusion, we report the first facile approach that successfully addresses the surface passivation of Mg metal in a simple salt electrolyte ($Mg(TFSI)_2$-DME) via formation of an Mg ion conductive surface layer by addition of iodine. The Mg anode/electrolyte interface was thoroughly investigated by various spectroscopic techniques in terms of its morphology, surface chemistry, and interfacial resistance. The facilitated Mg deposition/stripping could be explained by the formation of an Mg ion conducting surface layer containing magnesium iodide. The presence of such an Mg ion conducting layer enables Mg anode operation at low overpotential. The electrochemical cycling of an Mg/S full cell verifies the reduced cell voltage hysteresis well, and the charge/discharge curves of Mg/Mg/S three-electrode cell demonstrate that the reduced cell voltage hysteresis is attributed to the reduction of Mg deposition/stripping overpotentials. This approach renders this electrolyte, which is advantageous compared to complex Mg electrolytes for its easy preparation, better cathode compatibility, wide anodic stability, and high ionic conductivity, applicable for practical Mg metal batteries. More importantly, this work is the very first of its kind in the research of Mg battery electrolytes, one of the corner-stones for the realization of RMBs. Our findings point out that the surface chemistry and the composition of the SEI plays a major role in determining the Mg anode performance, and sheds light on the effects of additives. It also opens a new avenue for the development of simple electrolytes for RMBs.

Experimental Section

Cathode Fabrication: Activated carbon cloth/sulfur (denote as ACC/S or ACCS) cathode was prepared through a melt-diffusion method following previous reports.[16,33] The ACC samples (ACC-507-20) were obtained from Kynol Inc. (USA) and were cut to circular discs with a diameter of ≈8 mm. Elemental sulfur (99.98%, Sigma-Aldrich) was spread on the bottom of a stainless steel reactor and then ACC disks were laid on top of the sulfur powder. The reactor was then sealed in glovebox and heated to 155 °C for 12 h. Sulfur loading was measured by subtracting the mass of blank ACC from ACC/S. Typical sulfur loading is 0.8–1.0 mg cm^{-2} in this study.

Electrolyte Preparation: Electrolytes were prepared under pure argon atmosphere in a Braun, Inc. glovebox (<1 ppm of water and oxygen). The magnesium(II) bis(trifluoromethane sulfonyl)imide ($Mg[N(SO_2CF_3)_2]_2$, $Mg(TFSI)_2$) based electrolyte was synthesized following previously reported procedures.[29,34,35] The electrolytes were prepared by adding different ratios of iodine (I_2, ACS reagent, ≥99.8%, solid, Sigma-Aldrich) additive into the 0.5 M (mol L^{-1}) $Mg(TFSI)_2$-DME (1,2-dimethoxyethane, anhydrous, 99.5%, inhibitor-free, Sigma-Aldrich) based electrolyte. The prepared electrolytes were dried with 4 Å molecular sieves (beads, 8–12 mesh, Sigma-Aldrich) overnight before use.

Electrochemical Measurement: Galvanostatic charge/discharge tests were carried out in three-electrode T-cell and two-electrode Swagelok cell set-ups with an Arbin Instrument. The three-electrode T-cell consisted of ACC/S cathode as WE, Mg foil as both RE and CE, glass microfiber filters (Whatman, Grade GF/B) as separator, and prepared electrolyte with a voltage cut-off range of 1–2.5 V versus Mg/Mg^{2+}. Galvanostatic charge/discharge tests in an ACCS/Mg Swagelok full cell were performed with a voltage cut-off range of –0.5 to 3.0 V for blank electrolyte, 0.5–3.0 V for electrolyte with 1×10^{-3} M iodine additive, and 1.0–2.5 V for electrolyte with 5×10^{-3} and 50×10^{-3} M iodine additive. All Mg foils were thoroughly polished in Ar atmosphere by sand paper to remove all of the surface oxide layer and expose a fresh Mg surface. The specific capacity was normalized to the mass of sulfur in the composite cathode. The Mg stripping/deposition process was also conducted in the same T-cell set-up and with the same electrolytes with Mg/Mg/Mg symmetric electrodes at 1.41 mA cm^{-2} h^{-1}. Electrochemical impedance spectra were carried out on a Gamry Reference 3000 from 10^6 Hz to 0.1 Hz at an amplitude of 5 mV. All the electrochemical measurements were performed at room temperature.

Materials Characterization: The morphology and element composition of the materials were examined by a Hitachi SU-70 field-emission SEM and EDS. XPS analysis was measured with a Kratos AXIS Ultra DLD instrument using monochromated Al Kα X-rays as the excitation source. All the samples were rinsed several times to thoroughly remove the soluble species on the surface with DME solvent before characterization.

Supporting Information

Supporting Information is available from the Wiley Online Library or from the author.

Acknowledgements

X.L. and T.G. contributed equally to this work. This work was supported as part of the Nanostructures for Electrical Energy Storage (NEES), an Energy Frontier Research Center funded by the U.S. Department of Energy, Office of Science, Basic Energy Sciences under Award number DESC0001160. The authors acknowledge the support of the Maryland Nano Center and its AIM Lab. X.L. was financially supported by the China Scholarship Council while visiting the Department of Chemical and Biomolecular Engineering at University of Maryland, College Park.

Conflict of Interest

The authors declare no conflict of interest.

Keywords

electrochemistry, iodine additive, $Mg(TFSI)_2$-DME simple salt electrolyte, reduce overpotential, sulfur

Received: June 25, 2017
Revised: August 24, 2017
Published online:

[1] H. D. Yoo, I. Shterenberg, Y. Gofer, G. Gershinsky, N. Pour, D. Aurbach, *Energy Environ. Sci.* **2013**, *6*, 2265.
[2] R. Mohtadi, F. Mizuno, *Beilstein J. Nanotechnol.* **2014**, *5*, 1291.
[3] J. Muldoon, C. B. Bucur, T. Gregory, *Chem. Rev.* **2014**, *114*, 11683.
[4] I. Shterenberg, M. Salama, Y. Gofer, E. Levi, D. Aurbach, *MRS Bull.* **2014**, *39*, 453.
[5] Y. Cheng, H. J. Chang, H. Dong, D. Choi, V. L. Sprenkle, J. Liu, Y. Yao, G. Li, *J. Mater. Res.* **2016**, *31*, 3125.
[6] J. Muldoon, C. B. Bucur, T. Gregory, *Angew. Chem., Int. Ed.* **2017**, *56*, 2.
[7] P. Canepa, G. Sai Gautam, D. C. Hannah, R. Malik, M. Liu, K. G. Gallagher, K. A. Persson, G. Ceder, *Chem. Rev.* **2017**, *117*, 4287.
[8] D. Aurbach, Z. Lu, A. Schechter, Y. Gofer, H. Gizbar, R. Turgeman, Y. Cohen, M. Moshkovich, E. Levi, *Nature* **2000**, *407*, 724.
[9] O. Mizrahi, N. Amir, E. Pollak, O. Chusid, V. Marks, H. Gottlieb, L. Larush, E. Zinigrad, D. Aurbach, *J. Electrochem. Soc.* **2008**, *155*, A103.
[10] H. S. Kim, T. S. Arthur, G. D. Allred, J. Zajicek, J. G. Newman, A. E. Rodnyansky, A. G. Oliver, W. C. Boggess, J. Muldoon, *Nat. Commun.* **2011**, *2*, 427.
[11] Z. Zhao-Karger, X. Zhao, O. Fuhr, M. Fichtner, *RSC Adv.* **2013**, *3*, 16330.
[12] K. A. See, K. W. Chapman, L. Zhu, K. M. Wiaderek, O. J. Borkiewicz, C. J. Barile, P. J. Chupas, A. A. Gewirth, *J. Am. Chem. Soc.* **2016**, *138*, 328.
[13] P. Canepa, S. Jayaraman, L. Cheng, N. Rajput, W. D. Richards, G. Sai Gautam, L. A. Curtiss, K. Persson, G. Ceder, *Energy Environ. Sci.* **2015**, *8*, 3718.
[14] C. J. Barile, R. G. Nuzzo, A. A. Gewirth, *J. Phys. Chem. C* **2015**, *119*, 13524.
[15] C. J. Barile, E. C. Barile, K. R. Zavadil, R. G. Nuzzo, A. A. Gewirth, *J. Phys. Chem. C* **2014**, *118*, 27623.
[16] T. Gao, M. Noked, A. J. Pearse, E. Gillette, X. Fan, Y. Zhu, C. Luo, L. Suo, M. A. Schroeder, K. Xu, S. B. Lee, G. W. Rubloff, C. Wang, *J. Am. Chem. Soc.* **2015**, *137*, 12388.
[17] H. Tian, T. Gao, X. Li, X. Wang, C. Luo, X. Fan, C. Yang, L. Suo, Z. Ma, W. Han, C. Wang, *Nat. Commun.* **2017**, *8*, 14083.
[18] X. Sun, P. Bonnick, V. Duffort, M. Liu, Z. Rong, K. A. Persson, G. Ceder, L. F. Nazar, *Energy Environ. Sci.* **2016**, *195*, 6902.
[19] Z. Lu, A. Schechter, M. Moshkovich, D. Aurbach, *J. Electroanal. Chem.* **1999**, *466*, 203.
[20] I. Shterenberg, M. Salama, H. D. Yoo, Y. Gofer, J.-B. Park, Y.-K. Sun, D. Aurbach, *J. Electrochem. Soc.* **2015**, *162*, 7118.
[21] S. Terada, T. Mandai, S. Suzuki, S. Tsuzuki, K. Watanabe, Y. Kamei, K. Ueno, K. Dokko, M. Watanabe, *J. Phys. Chem. C* **2016**, *120*, 1353.
[22] J. G. Connell, B. Genorio, P. P. Lopes, D. Strmcnik, V. R. Stamenkovic, N. M. Markovic, *Chem. Mater.* **2016**, *28*, 8268.
[23] N. N. Rajput, X. Qu, N. Sa, A. K. Burrell, K. A. Persson, *J. Am. Chem. Soc.* **2015**, *137*, 3411.
[24] N. Sa, N. N. Rajput, H. Wang, B. Key, M. Ferrandon, V. Srinivasan, K. A. Persson, A. K. Burrell, J. T. Vaughey, *RSC Adv.* **2016**, *6*, 113663.
[25] I. Shterenberg, M. Salama, H. D. Yoo, Y. Gofer, J.-B. Park, Y.-K. Sun, D. Aurbach, *J. Electrochem. Soc.* **2015**, *162*, A7118.
[26] O. Tutusaus, R. Mohtadi, N. Singh, T. S. Arthur, F. Mizuno, *ACS Energy Lett.* **2017**, *2*, 224.
[27] V. Fournier, P. Marcus, I. Olefjord, *Surf. Interface Anal.* **2002**, *34*, 494.
[28] A. Hanom Ahmad, F. S. Abdul Ghani, *AIP Conf. Proc.* **2009**, *1136*, 31.
[29] S. Ha, Y. Lee, S. W. Woo, B. Koo, J. Kim, J. Cho, K. T. Lee, N. Choi, *ACS Appl. Mater. Interfaces* **2014**, *6*, 4063.
[30] N. Sa, H. Wang, D. L. Proffit, A. L. Lipson, B. Key, M. Liu, Z. Feng, T. T. Fister, Y. Ren, C.-J. Sun, J. T. Vaughey, P. A. Fenter, K. A. Persson, A. K. Burrell, *J. Power Sources* **2016**, *323*, 44.
[31] Y. Orikasa, T. Masese, Y. Koyama, T. Mori, M. Hattori, K. Yamamoto, T. Okado, Z.-D. Huang, T. Minato, C. Tassel, J. Kim, Y. Kobayashi, T. Abe, H. Kageyama, Y. Uchimoto, *Sci. Rep.* **2014**, *4*, 5622.
[32] Z. Zhao-Karger, X. Zhao, D. Wang, T. Diemant, R. J. Behm, M. Fichtner, *Adv. Energy Mater.* **2015**, *5*, 1401155.
[33] T. Gao, X. Li, X. Wang, J. Hu, F. Han, X. Fan, L. Suo, A. J. Pearse, S. B. Lee, G. W. Rubloff, K. J. Gaskell, M. Noked, C. Wang, *Angew. Chem., Int. Ed.* **2016**, *55*, 9898.
[34] K. W. Nam, S. Kim, S. Lee, M. Salama, I. Shterenberg, Y. Gofer, J.-S. Kim, E. Yang, C. S. Park, J.-S. Kim, S.-S. Lee, W.-S. Chang, S. G. Doo, Y. N. Jo, Y. Jung, D. Aurbach, J. W. Choi, *Nano Lett.* **2015**, *15*, 4071.
[35] A. Baskin, D. Prendergast, *J. Phys. Chem. C* **2016**, *120*, 3583.

